Object Detection Probability for Highly Automated Vehicles: An Analytical Sensor Model

Florian Alexander Schiegg[1,2], Ignacio Llatser[2] and Thomas Michalke[3]

[1]*Institute of Communications Technology, Leibniz University of Hannover, Appelstraße 9A, Hannover, Germany*
[2]*Robert Bosch GmbH, Corporate Research, Robert-Bosch-Strasse 200, Hildesheim, Germany*
[3]*Robert Bosch GmbH, Corporate Research, Robert-Bosch-Campus 1, Renningen, Germany*

Keywords: Sensor Model, Object Detection, Advanced Driver Assistance Systems, Collective Perception, V2X, Environmental Model, Highly Automated Driving, Cooperative Awareness.

Abstract: Modern advanced driver assistance systems (ADAS) increasingly depend on the information gathered by the vehicle's on-board sensors about its environment. It is thus of great interest to analyse the performance of these sensor systems and its dependence on macroscopic traffic parameters. The work at hand aims at building up an analytical model to estimate the number of objects contained in a vehicle's environmental model. It further considers the exchange of vehicle dynamics and sensor data by vehicle-to-vehicle (V2X) communication to enhance the environmental awareness of the single vehicles. Finally, the proposed model is used to quantify the improvement in the environmental model when complementing sensor measurements with V2X communication.

1 INTRODUCTION

The increasing road traffic automation has come along with the need for highly reliable environmental models of the automated vehicle's surroundings. In order to be able to assist the driver or even take decisions themselves, vehicles have to perceive their surroundings and detect possible dangers and hazards as precisely as possible.

To this end, the data recorded by the vehicle's on-board sensors, like video cameras, radars or LIDARs is aggregated by making use of association algorithms like the Joint Probabilistic Data Association (JPDA) (Rezatofighi, et al., 2015) and subsequently filtered and fused by algorithms such as Kalman or Particle filters (Chen, 2003). All of these algorithms sensitively depend on the accuracy of the processed sensor data. The more data is available about an object, the more precisely its current state may be determined. Once a new object is detected and validated this way, it is incorporated into the vehicle's environmental model. As long as the object stays within the vehicle's Field-of-View (FOV), it is kept in the environmental model and its state is periodically updated until it is no longer perceived for a certain time.

However, one of the main limitations of current on-board object detection sensors is the shadowing of the FOV by obstacles and traffic objects in the vicinity. To mitigate this impairment, Vehicle-to-Everything (V2X) communication has been receiving increasing interest lately. By sharing information of their local environmental models with neighbouring vehicles, V2X-capable vehicles are able to significantly increase their knowledge about their surroundings. The environmental model arising from including V2X-Data into the local environmental model (LEM) is commonly referred to as the global environmental model (GEM). It not only allows to substantially enhance the accuracy of the managed data, but it may also include objects that are out of the sensor's Line-of-Sight (LOS) and thus not contained within the LEM. Nevertheless, the GEM may still be incomplete or even faulty. Hence, it is of great importance for automated vehicles to be able to estimate the accuracy of the environmental model at the time they are facing a decision. Below a model is derived analytically, that aims at determining the number of objects known to the vehicle based on (i) its own sensors and (ii) V2X communication with vehicles in its vicinity. It is then demonstrated on the example of a highway scenario.

2 RELATED WORK

Considerable effort has been conducted in developing more efficient object detection and tracking algorithms for specific sensors or combinations of them. An extensive overview is given by (Sivaraman, 2013). Empirical studies were performed for some of these algorithms, to investigate the detection probability given specific scenarios (Held, Levinson, & Thrun, 2012). Geese et. al. (2018) recently presented an approach to predict the performance of an optical sensor in dependence of the environmental conditions. Another approach is the detection and tracking of moving objects (DATMO) based on occupancy grids as presented, e.g. by Baig, Vu, & Aycard (2009). However, to the best of the authors' knowledge, no thorough theoretical analysis about the number of detectable objects or the fraction of objects contained in the LEM or the GEM has been conducted so far.

The contribution of the present work is an analytical model that allows estimating the absolute and the relative amount of objects contained in both LEM and GEM, in dependence of macroscopic parameters, such as the linear vehicle density, and the properties of road, vehicles and sensors.

3 VEHICLE PERCEPTION

In order to perceive their environment, automated vehicles have to make use of all kinds of sensors. While subsection 3.1 deals with the vehicle's own on-board sensors, subsection 3.2 introduces the concepts of cooperative awareness and collective perception, which allow utilizing the data of external sensors shared through V2X communication.

3.1 On-board Sensors

The growing complexity of advanced driver assistance systems (ADAS) is leading to an increasing number of sensor-systems being installed in nowadays' vehicles. Fig. 1 shows some of them. They can roughly be divided into four classes, depending on their range: (i) ultra-short (up to 5 m): e.g. ultrasound for parking assistance, (ii) short (~30 m): e.g. radar for blind spot detection, rear collision warning or cross traffic alert, (iii) mid-range (~100 m): e.g. radar, LIDAR or video for surround view, object detection, video-supported parking assistance, traffic sign recognition, lane departure warning, emergency braking or collision avoidance, and (iv)

long range (~200 m): radar e.g. for adaptive cruise control or sheer-in assistance on a highway.

To ensure the functional safety of highly automated vehicles, sensor redundancy for object detection will be necessary, making sure the vehicle is still able to deal with adverse environmental conditions or even a sensor system falling out.
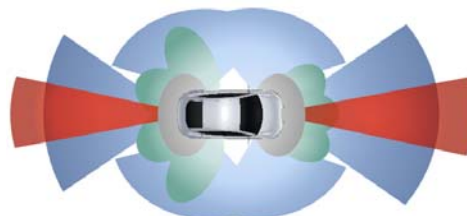

Figure 1: Vehicle sensors of ultra-short (grey), short (green), medium (blue) and long range (red).

The LEM is essentially based on data registered by the mid- and long-range sensors. To detect objects that are further away, V2X communication is of great use.

3.2 V2X Communication

The limited perception capabilities of on-board sensors can be enhanced with V2X communication, by means of cooperative awareness and collective perception. Cooperative awareness consists of vehicles transmitting data about their own state via V2X communication, such as their current position, speed and heading. This service is implemented by the Cooperative Awareness Message (CAM) in Europe and by the Basic Safety Message (BSM) in the US. Collective perception (Günther, 2016) allows cars to inform nearby vehicles of objects detected by their own on-board sensors. The exchange of Collective Perception Messages (CPM) enables vehicles to perceive objects beyond their own sensor's range by looking through other vehicles' "eyes". The collective perception service is currently considered for standardization by the European Telecommunications Standards Institute (ETSI) in order to ensure its interoperability among all equipped vehicles.

4 ANALYTICAL MODEL

The quality of a highly automated vehicle's environmental model sensitively depends on the fraction of objects it contains. It is thus necessary to predict this quantity as accurately as possible. With

this goal, an analytical model based on the specifications of the vehicle dimensions, their on-board sensors, the vehicle density and the scenario characteristics is set up. The model should further consider occlusion by other vehicles, which becomes especially relevant at higher vehicle densities as shown in the figure below, and V2X communication among the vehicles.
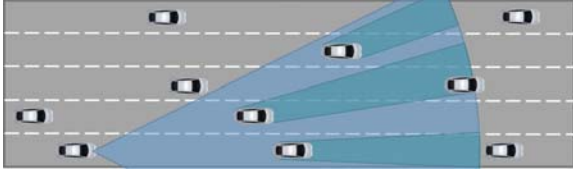

Figure 2: Top view of a vehicle on a highway equipped with a free-field sensor to detect traffic objects in its vicinity. The NLOS section of the FOV (blue area) is indicated in cyan.

Finally, it would be desirable for the model to be as independent of a concrete vehicle distribution as possible, depending only on macroscopic parameters such as the average vehicle velocity, density, dimension and V2X penetration rate.

4.1 Objects in Field of View

The number of objects contained in a sensor's FOV (marked in blue in Fig. 2) is given by

$$n_{\text{obj}} = \sum_{n=1}^{N} n_{\text{obj}}^{n} \qquad (1)$$

where N and n_{obj}^{n} are the number of lanes within the sensor's FOV and the number of vehicles on lane n within the FOV respectively. The latter is defined by the vehicle distribution $p_n(x)$ between the boundaries L_n^- and L_n^+ (see example in Fig. 4) of the FOV on line n:

$$n_{\text{obj}}^{n} = \int_{L_n^-}^{L_n^+} p_n(x)dx \qquad (2)$$

While the position of the analyzed vehicle, further referred to as ego-vehicle, does have a significant influence on the vehicle distribution on its own lane, its effect on the distribution of vehicles on other lanes is almost negligible (Filzek & Breuer, 2001). The vehicle distribution can thus be assumed as isotropic on each of these lanes and corresponds to their vehicle densities σ_n:

$$p_n(x) = \sigma_n \qquad (3)$$

On the ego-lane however, the distribution is characterized by the exact localization of the ego-vehicle. The distribution function on the ego-lane is thus composed of the distribution functions $p_{\text{ego}}^i(x)$ of every vehicle i on the ego-lane within the sensors FOV

$$p_{\text{ego}}(x) = \sum_i p_{\text{ego}}^i(x) \qquad (4)$$

with the mean of $p_{\text{ego}}^i(x)$ having to fulfill

$$\langle x_i \rangle = \int x\, p_{\text{ego}}^i(x)\, dx \overset{!}{=} i\, \sigma_{\text{ego}}^{-1} \qquad (5)$$

While the distribution of the ego-vehicle equals a simple Dirac delta function at the origin

$$p_{\text{ego}}^0(x) = \delta \qquad (6)$$

the distributions of the neighbouring vehicles have variance, skewedness and kurtosis that depend on the mean vehicle density σ_{ego} and velocity v_{ego} on the ego-lane and follow the relation

$$p_{\text{ego}}^{\pm 1}(x, \sigma_{ego}, v_{ego}) = l_{\text{veh}} + d_{\text{int}}(\pm x, \sigma_{ego}, v_{ego}) \qquad (7)$$

where l_{veh} and d_{int} are the mean vehicle length and the inter-vehicle distance respectively. Numerous studies have been conducted about the latter in the past (Filzek & Breuer, 2001). By convolution, it is then possible to recursively obtain the remaining vehicle distribution functions:

$$p_{\text{ego}}^{i\pm 1}(x) = (p_{\text{ego}}^i * p_{\text{ego}}^{\pm 1})(x) \qquad (8)$$

Fig. 3 shows a vehicle distribution around the ego-vehicle. As expected, $p_{\text{ego}}(x)$ quickly tends towards σ_{ego} for $i \geq 2$ vehicles away from the ego-vehicle.
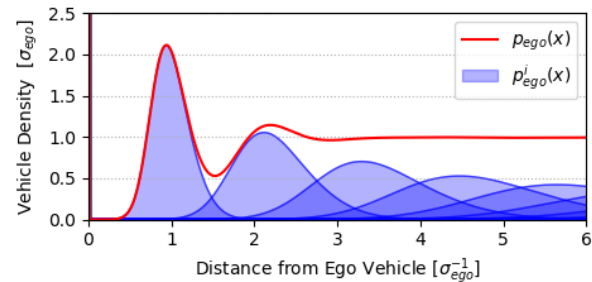

Figure 3: Vehicle distribution on ego-lane. The ego-vehicle itself is represented by a Dirac-function at the origin.

Putting together Eq. 1, 2 and 3 one obtains

$$n_{\text{obj}} = \sum_{n=1}^{N} \int_{L_n^-}^{L_n^+} p_n(x) dx \qquad (9)$$
$$= n_{\text{obj}}^{\text{ego}} + \sum_{n \neq \text{ego}}^{N} \sigma_n L_n \overset{R \gg \sigma_{\text{ego}}^{-1}}{\approx} \sum_{n=1}^{N} \sigma_n L_n$$

where L_n is the length of the lane segment of lane n within the FOV of the sensor and R is the sensor's range. Fig 4 exemplarily shows L_2 corresponding to the distance between L_2^- and L_2^+. In general, for a given sensor, L_n can be determined from the sensor's specifications. However, it can also easily be determined by making use of sensor parameters, such as its offset relative to the ego-vehicle's front axis $\delta = (\delta_x | \delta_y)$, its already introduced range R and the angles ϑ^- and ϑ^+ delimiting its frustum.

4.2 Objects in Line of Sight

Usually a relevant fraction of the vehicles in the sensor's FOV will be hidden behind closer objects. These Non-Line-of-Sight (NLOS) segments are depicted in red in the figure below (somewhat shorter in range for a better visualization).
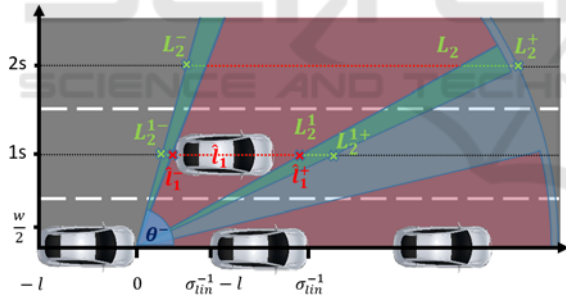

Figure 4: Schematic representation of a sensor's Line-of-Sight and Non-Line-of-Sight segments.

In analogy to Eq. 9, the number of objects within LOS (green and blue segments in the figure above) is:

$$n_{\text{LOS}} = \sum_{n=1}^{N} \int_{\text{LOS}} p_n(x) dx = n_{\text{LOS}}^{\text{ego}} + \sum_{n \neq \text{ego}}^{N} \sigma_n L_{\text{LOS}}^n \quad (10)$$

L_{LOS}^n being the overall length of all lane sub-segments on lane n that are in LOS.

Even though the vehicle may perceive further objects on the ego-lane (e.g. due to misaligned vehicles, different vehicle sizes or through the front vehicle windows) the detection accuracy generally will not be good enough to extract the necessary information (e.g. to fill all the mandatory CPM object fields). Thus, further detections on the ego-lane are negligible. With this the expectancy value of detectable objects $n_{\text{LOS}}^{\text{ego}}$ equivalents $n_{\text{obj}}^{\text{ego}}$ capped on one in both directions:

$$n_{\text{LOS}}^{\text{ego}} = \begin{cases} n_{\text{obj}}^{\text{ego}} & n_{\text{obj}}^{\text{ego}} < 1 \\ 1 & n_{\text{obj}}^{\text{ego}} \geq 1 \end{cases} \qquad (11)$$

For instance, the second term of Eq. 10 may be developed as follows

$$\sum_{n \neq \text{ego}}^{N} \sigma_n L_{\text{LOS}}^n = \sum_{n \neq \text{ego}}^{N} \sigma_n \rho_n L_n \qquad (12)$$

where ρ_n represents the fraction of visibility to lane n. The LOS fraction can take values from zero (if no LOS is available) to one (when there are no occluding vehicles). It is composed of the LOS-fractions of all the lines between the ego-lane $i = 0$ and the target lane $i = n$ and can be computed as:

$$\rho_{n \neq \text{ego}} = \prod_{i=1}^{n-1} \rho_n^{(i)} \qquad (13)$$

Shadowing caused by vehicles on the ego-lane reduces visibility towards the target lane. It may only change the upper boundary of L_{LOS}^n. A geometric analysis allows to calculate the expectancy value of the last visible point on lane n

$$L_{n,\text{LOS}}^{(0)+} = \int_{x=0^+}^{\langle x \rangle = \frac{1}{2}} p_{\text{ego}}(x) \left(\delta_x + x \frac{ns - \delta_y}{\omega/2 - \delta_y} \right) dx \quad (14)$$

where ω and s are the widths of the vehicle and the lanes respectively. Eq. 10 can easily be resolved using Eq. 4 and 5. Considering only vehicles on the ego-lane, the LOS section of lane n may thus be expressed as:

$$L_{n,\text{LOS}}^{(0)} = \min(L_{n,\text{LOS}}^+ , L_{n,\text{LOS}}^{(0)+}) - L_n^- \qquad (15)$$

At higher distances from the ego-lane, the number of vehicles occluding the vision will increase. However, objects on lanes in between may interfere in the LOS only if they are placed between the sensor and its theoretical visibility area on lane n (shown in green in Fig. 4). Let's define $L_n^{(i)}$ as the portion of lane i where vehicles could shadow lane n. As an example, L_2^1 is shown in Fig 4, comprising the segment from L_2^{1-} to L_2^{1+}. A simple geometrical analysis yields:

$$L_n^{(i)} = \left(\frac{is - \delta_y}{ns - \delta_y} \right) L_n \qquad (16)$$

The fraction of visibility on this line can now be determined by

$$\rho_n^{(i)} = \left(1 - \frac{n_{\text{shad}}^{i/n}(L_n)\bar{l_i}}{L_n^{(i)}} \right) \qquad (17)$$

where $n_{\text{shad}}^{i/n}$ stands for the number of vehicles on line i interfering the LOS to lane n and $\bar{l_i}$ is their average effective cross-section. Knowing that the x-position relative to the ego-vehicle is not correlated (see Section 4.1), $\bar{l_i}$ can be computed as

$$\bar{l_i} = \int_{L_n^{i-}-l}^{L_n^{i+}} \frac{\hat{l_i}(x)}{L_n^{(i)}} dx \qquad (18)$$

with $\hat{l_i}(x)$ representing the projection of a vehicle at position x on the center of lane i. For the sake of simplicity, the sensor offset is omitted in Eq. 19 and 20, however it can easily be reincorporated

$$\hat{l_i} = \begin{cases} a(x) & L_n^{i-} - l \le x < L_n^{i-} \\ a(x) - b(x) & L_n^{i-} \le x < L_n^{i+} - l \\ L_n^{(i)} - b(x) & L_n^{i+} - l \le x < L_n^{i+} \end{cases} \qquad (19)$$

with the terms $a(x) = \frac{(x+l)ns}{ns-w/2}$ and $b(x) = \frac{xns}{ns+w/2}$. Reincorporating this into Eq. 18 and solving the integral yields:

$$\bar{l_i} = \int_{L_n^{i-}-l}^{L_n^{i+}} \frac{\hat{l_i}(x)}{L_n^{(i)}} dx = l + \frac{L_n i \left(\frac{w}{s} \right)}{2n^2 - 0.5 \left(\frac{w}{s} \right)^2} \qquad (20)$$

Subsequently the number of shadowing vehicles on the earlier lines $n_{\text{shad}}^{i/n}$ has to be determined for Eq. 17. It can be computed by the recursive equation:

$$\begin{aligned} n_{\text{shad}}^{i/n} &= \sigma_n L_n^{(i)} \rho_n \\ &= \sigma_n L_n^{(i)} \prod_{k=1}^{i-1} \rho_n^{(k)} \\ &= \sigma_n L_n^{(i)} \prod_{k=1}^{i-1} \left(1 - \frac{n_{\text{shad}}^{k/n}(L_n)\bar{l_i}}{L_n^{(k)}} \right) \end{aligned} \qquad (21)$$

Due to the relation $n_{\text{LOS}}^n = n_{\text{shad}}^{n/n}$ the expectancy value of detectable vehicles on lane n can finally be written as:

$$n_{\text{LOS}}^n = \sigma_n L_n \prod_{i=1}^{n-1} \left(1 - \frac{n_{\text{shad}}^{i/n}(L_n)\bar{l_i}}{L_n^{(i)}} \right) \qquad (22)$$

It should be noted that this is not equal to the number of vehicles shadowing line $m > n$, since only $L_m^{(n)}/L_n^{(n)}$ of these vehicles will interfere the LOS to line m.

4.3 Objects Detected by V2X Communication

Vehicles not detectable by on-board sensors can still be detected via V2X communications, by means of cooperative awareness and collective perception (see Section 3.2). These services make it possible to extend the own vehicle's Local Environmental Model (LEM) to an enhanced Global Environmental Model (GEM), which includes vehicles detected by means of V2X communication in addition to those detected by the vehicle's on-board sensors. The total number of vehicles in the GEM can be expressed as:

$$n_{\text{Tot}} = n_{\text{LOS}} + n_{\text{V2X}} \qquad (23)$$

Knowing that a car is detectable via on-board sensors by n_{LOS} vehicles, one can compute the probability that at least one of these vehicles is V2X-equipped, and thus able to inform the ego-vehicle about the detected car

$$p_{\text{V2X}} = 1 - (1 - \varphi)^{n_{\text{LOS}}+1} \qquad (24)$$

where the $+1$ comes from the transmitting vehicle sharing its own state through a CAM, a CPM or any other V2X-message and φ being the V2X penetration rate. With this, it is now possible to determine the expectancy value of vehicles detected merely by V2X communication:

$$n_{\text{V2X}} = (n_{\text{Obj}} - n_{\text{LOS}})(1 - (1 - \varphi)^{n_{\text{LOS}}+1}) \qquad (25)$$

5 RESULTS AND DISCUSSION

In this section, the theoretical model is demonstrated and discussed on the example of a highly autonomous vehicle on a straight highway segment. It is divided into two sections, dealing with the LEM (Section 5.1) and the GEM (Section 5.2) respectively. Different performance metrics are analysed in dependence of the vehicle density, the number of lanes, the V2X penetration rate and the utilized sensor system. Due

to its depreciable effect on the normalized vehicle distribution (Fig. 3) and its strong correlation to the vehicle density (Filzek & Breuer, 2001), the vehicle velocity is not further investigated.

5.1 Local Environmental Model

Even though the presented analytical model already builds on a number of simplifications, for demonstration purposes a few more have to be introduced. Below, they are presented together with the necessary set of parameters:

- Highly autonomous vehicles require a full perception of their environment in order to act and react according to it. Thus, a full surround view is indispensable.
- Sensor redundancy significantly increases the reliability of the system. For this reason, full-surround video, LIDAR, and radar systems, with front and rear ranges of 100 m (video), 120 m (LIDAR) and 180 m (radar) are discussed.
- Even though side sensors will have a much lower range than their front and rear peers, it will be sufficient to cover the full street width.

- To reduce the number of variables a constant vehicle density is presumed for the purposes of this analysis.
- The vehicle length and width are set to 4.4 m and 1.8 m respectively, corresponding to the average dimensions of vehicles sold in Germany in 2018 (Centre for Automotive Research (CAR) of the Duisburg-Essen University, 2018).
- The lane width was set to 3.5 m as defined in the German RQ26, RQ33 and RQ10.5 highway standards by the FGSV (1982).

Fig. 5 shows the results of the postulated model for a) the video-, b) the LIDAR-, and c) the radar-system on a four-lane highway. The x- and y-axes of the upper three plots represent the ego-lane and the vehicle density respectively.

As could be expected, cars on the centre lanes detect more vehicles than those on outer ones. Moreover, the number of detectable objects reaches a maximum for a certain vehicle density. The location of this maximum further depends on the range of the sensor system. Apparently, a higher range shifts the maximum down to lower densities. This can easily be explained, considering that the inter-vehicle distance increases with decreasing vehicle density.
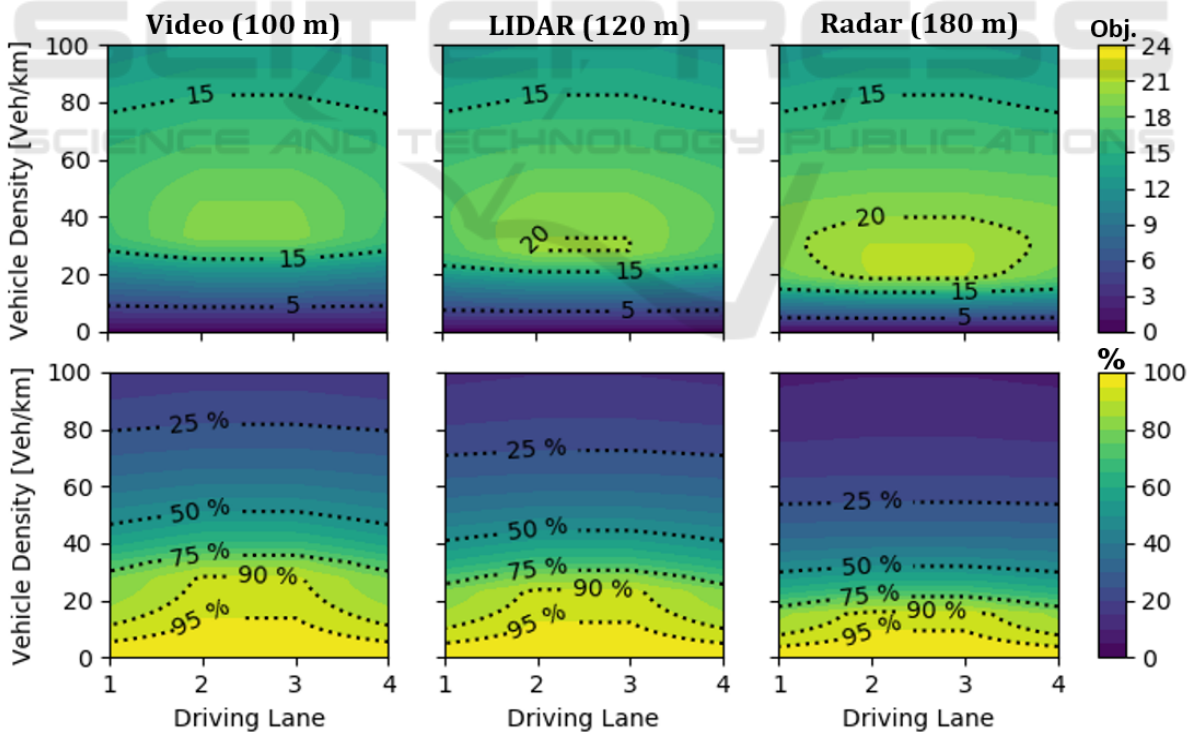

Figure 5: Expected object detections (above) and Environment Awareness Ratio (EAR, bellow) of a vehicle depending on its actual driving lane on a 4-lane highway and the average linear vehicle density for different full surround sensor systems.
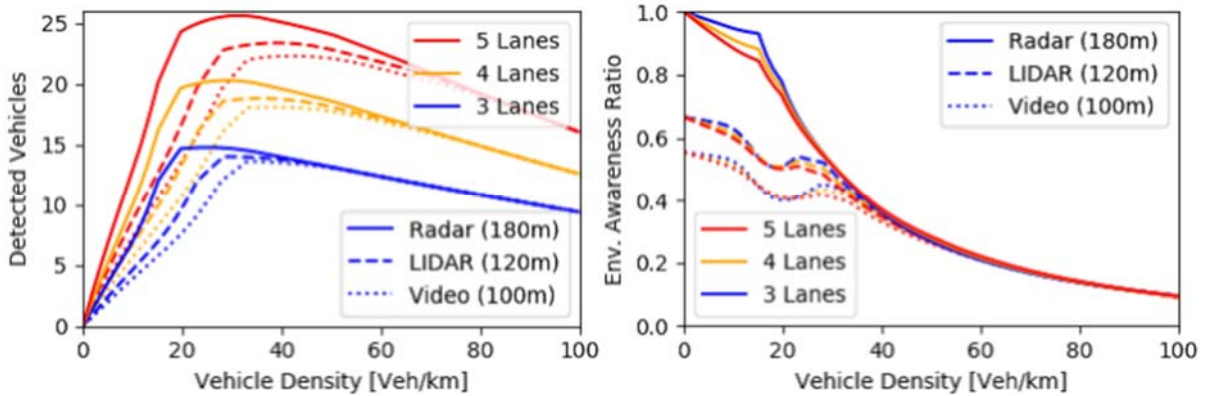
Figure 6: Vehicles in LOS (left) and Environmental Awareness Ratio (EAR, right) of a vehicle depending on the number of highway-lanes and the vehicle density for full surround video, LIDAR and radar systems.

At low inter-vehicle distances, the number of detected vehicles will not increase significantly with increasing sensor range, since shadowing by cars in the proximity dominates. However, at lower vehicle densities, vehicles that are further away may also be detected. The maxima are located at densities of approximately 38 (video), 32 (LIDAR) and 21 (radar) vehicles per kilometre. This corresponds to average inter-vehicle distances of 22 m, 27 m and 41 m respectively, proving the direct correlation with the range of the sensor system.

Besides the number of detectable vehicles, also the Environmental Awareness Ratio (EAR) i.e. the detection probability of an object within the FOV is of great interest. It can be determined as follows:

$$\text{EAR} = \frac{n_{\text{LOS}}}{n_{\text{obj}}} \quad (26)$$

The lower row of Fig. 5 shows the environmental awareness ratio for a) the video-, b) LIDAR-, and c) radar system. As can be seen, the number of detectable objects decreases at lower densities, however, the awareness ratio improves due to the lack of shadowing vehicles in the vicinity. For this reason, the EAR is essential to complement the number of detectable objects.

To investigate the effect of the number of lanes on the number of detectable objects, the latter was determined for highways of 3, 4, and 5 lanes as an average over each of their lanes for the three investigated sensor systems (Fig. 6, left). It is worth noticing that the maximal amount of detectable vehicles always moves towards higher densities with increasing number of lanes. Moreover, the previous findings of the four-lane highway seem to hold accordingly for the three- and five-lane highways.

Opposed to the EARs of Fig. 5, which were normed on the ranges of each sensor system, the EARs in Fig. 6 (right) take the range of the radar system as reference. This allows to directly compare the performances of the three sensor systems. As was to be expected, the radar system clearly outperforms the radar and video systems at vehicle densities of up to 20 vehicles per kilometre due to its higher range. However, in the region between 20 and 40 vehicles per kilometre the performance gap closes quickly, and almost fully vanishes for densities over 40 vehicles per kilometre. Another interesting, yet expectable finding is that the number of lanes has a much smaller effect on the EAR. The addition of further lanes only leads to a slight deterioration of the vehicle's environmental awareness. Finally, the fast drop in EAR with the vehicle density down to around 10% at a density of 100 vehicles per kilometre clearly emphasises the need for an enhancement of the LEM.

5.2 Global Environmental Model

To investigate the GEM, further assumptions and simplifications are made:

- The channel capacity is expected to be high enough to avoid channel congestion.
- The communication range is assumed high enough to cover double the sensor range. Considering current technologies, e.g. LTE-V2X, IEEE 802.11p and the upcoming 5G-V2X, the communication range should not be a limiting factor on a highway scenario (Molina-Masegosa, 2017)
- The number of transmitted objects per CPM is limited to 20 to control the message size.

Fig. 7 shows the results for V2X penetration rates of 0% ($n_{\text{Tot}} = n_{\text{LOS}}$) to 100% ($n_{\text{Tot}} = n_{\text{obj}}$) for a five-
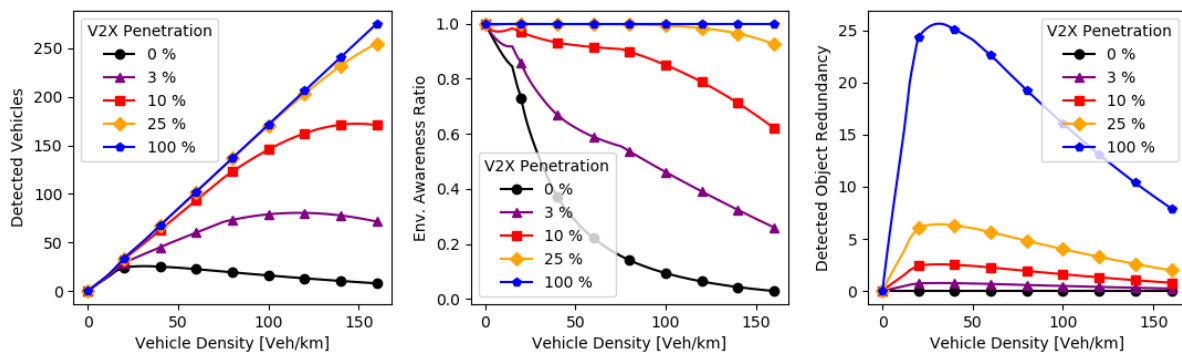
Figure 7: Expected number of vehicles contained in a vehicle's GEM (left), Environmental Awareness Ratio (EAR, middle), and Detected Object Redundancy (DOR, right) depending on the V2X penetration rate for a five-lane highway (Radar).

lane highway scenario. Clearly, collective perception significantly increases the number of detected objects (left) and hence the environmental awareness (middle) already at penetration rates of $\varphi = 3 - 10\%$. Only at very small inter-vehicle distances of around 2.5 m ($\sigma \approx 140$ Veh/km) the EAR decreases to ~75% and ~96% for $\varphi = 10\%$ and $\varphi = 25\%$ respectively, making higher penetration rates necessary. However, higher penetration rates also increase the Detected Object Redundancy (DOR, Fig.7, right). While a penetration rate of $\varphi = 10\%$ implies an expected detection redundancy of at most 3 objects for an EAR of at least 75%, the DOR increases up to 7 and 27 for penetration rates of $\varphi = 25\%$ and $\varphi = 100\%$ respectively. Specially the increase from $\varphi = 25\%$ to $\varphi = 100\%$ brings low profit ($\Delta EAR \approx 4\%$) at a high price ($\approx 400\%$ more transmitted data), suggesting the need for regulation mechanisms at higher V2X penetration rates.

6 CONCLUSION

The present work introduced an analytical model to determine the number of vehicles within the FOV of a sensor or a complete sensor system and the respective LOS fraction. The latter is important to estimate the quality of the LEM. It was found, that the environmental awareness ratio suffers a significant drop at denser traffic scenarios, making the exchange of data through V2X communication necessary. The integration of V2X services, such as cooperative awareness and collective perception, led to a significant enhancement of the environmental awareness already at very low V2X penetration rates. Higher penetration rates further increased the EAR; however, the gain was small in comparison to the rise in transmitted data.

The model builds a good analytical basis, not only for the better understanding of current and future sensor systems, but also for the development of V2X services like the CPM and the corresponding congestion control mechanisms.

REFERENCES

Baig, Q., Vu, T.-D., and Aycard, O. (2009). Online localization and mapping with moving objects detection in dynamic outdoor environments. *IEEE 5th International Conference on Intelligent Computer Communication and Processing* (pp. 401-408). IEEE.

Centre for Automotive Research (CAR) of the Duisburg-Essen University. (2018, May 07). WACHSTUM - Die Autos werden immer dicker. *Der Standard*.

Chen, Z. (2003). Bayesian Filtering: From Kalman Filters to Particle Filters, and Beyond. *Statistics, 182*(1), 1-69.

Filzek, B., and Breuer, B. (2001). *Distance behavior on motorways with regard to active safety ~ A comparison between adaptive-cruise-control (ACC) and driver.* SAE Technical Paper (No. 2001-06-0066).

Forschungsgesellschaft für Straßen- und Verkehrswesen (FGSV). (1982). *Richtlinien für die Anlage von Straßen: (RAS) / Forschungs-gesellschaft für Straßen- und Verkehrswesen, Arbeitsgruppe Straßenentwurf; Teil (RAS-Q): Querschnitte.* Köln: Forschungsgesellschaft für Straßen- und Verkehrswesen, Vol. 295.

Geese, M., Ulrich, S., and Alfredo, P. (2018). Detection Probabilities: Performance Prediction for Sensors of Autonomous Vehicles. *Electronic Imaging 2018 (17)*, 1-14.

Günther, H. J. (2016). Realizing collective perception in a vehicle. *Vehicular Networking Conference (VNC)* (pp. 1-8). IEEE.

Held, D., Levinson, J., and Thrun, S. (2012). A probabilistic framework for car detection in images using context and scale. *In Robotics and Automation (ICRA)* (pp. 1628-1634). IEEE International Conference.

Molina-Masegosa, R. and. (2017). LTE-V for sidelink 5G
V2X vehicular communications: a new 5G technology
for short-range vehicle-to-everything communications.
IEEE Vehicular Technology Magazine 12(4) (pp. 30-
39). IEEE.

Rezatofighi, S. H., Milan, A., Zhang, Z., Shi, Q., Dick, A.,
and Reid, I. (2015). Joint probabilistic data association
revisited. *IEEE International Conference on Computer
Vision (ICCV)* (pp. 3047-3055). IEEE.

Sivaraman, S. and. (2013). Looking at vehicles on the road:
A survey of vision-based vehicle detection, tracking,
and behavior analysis. *IEEE Trans-actions on
Intelligent Transportation Systems, 14(4)* (pp. 1773-
1795). IEEE.